JMEPEG (1996) 5:521-525

Modeling of Phase Transformation Behavior in Hot-Deformed and Continuously Cooled C-Mn Steels

Z. Liu, G. Wang, and W. Gao

Computer models of phase transformation from austenite to ferrite, austenite to pearlite, and austenite to bainite in hot-deformed carbon-manganese steels during continuous cooling were established on the basis of Cahn's transformation theory, thermal-dilatometric experiments, and thermodynamic calculations. These models showed good agreement with results measured from pilot hot rolling experiments.

Keywords
austenite, bainite, carbon-manganese steels, computer model, ferrite, pearlite, phase transformation

1. Introduction

MECHANICAL properties of hot-rolled steels are strongly influenced by their microstructure. Therefore, modeling of phase transformation from hot-deformed austenite (γ) to ferrite (α), pearlite (P), and bainite (B) is a powerful method to control microstructure of steels and improve their mechanical properties. This topic has become one of the most important research fields in physical metallurgy of steels in recent years (Ref 1). However, because the effects of hot deformation on phase transformation behavior are very complex, mathematical models of phase transformation from work-hardened γ were usually established by regression with experimental data. These regression models are not accurate enough and can only be used over a small range that depends on the experimental data.

In the present research, based on Cahn's phase transformation theory, dilatometric experiments, and thermodynamic calculations, we have developed computer models of phase transformations from hot-deformed γ to α, P, and B for carbon-manganese steels. The phase fractions calculated by using these models showed good agreement with experimentally measured results.

2. Modeling and Experimental Methods

2.1 *Phase Transformation Kinetic Models*

Cahn's phase transformation theory (Ref 2) and Scheil's additive rule (Ref 3) were applied to $\gamma \rightarrow \alpha$, $\gamma \rightarrow$ P, and $\gamma \rightarrow$ B transformations during continuous cooling. At the early stage of $\gamma \rightarrow \alpha$ transformation, the transformation takes place according to the mechanism of nucleation and growth:

$$\frac{dX_{F_1}}{dt} = 4.046(I_S S_\gamma)^{1/4} G_F^{1/4} \left(\ln \frac{1}{1-X}\right)^{3/4} (1-X) \qquad \text{(Eq 1)}$$

Z. Liu, G. Wang, and **W. Gao,** Department of Chemical & Materials Engineering, The University of Auckland, New Zealand.

where X_{F_1} is the transformed fraction of α-phase at early $\gamma \rightarrow \alpha$ transformation stage, X is the total transformed fraction of α, S_γ is the surface area of γ-grains in unit volume (cm^{-1}), G_F is the growth rate of α, and I_S is the nucleation rate of α, which can be computed according to the method given by Aaronson et al. (Ref 4):

$$I_S = K_1 T^{-1/2} D_C \exp\left(-\frac{K_2}{(RT\Delta G_V^2)}\right) \qquad \text{(Eq 2)}$$

where D_C is the diffusivity of carbon in γ, ΔG_V is the free energy change in unit volume for nucleation of α-phase ($J/mol/cm^3$), T is the absolute temperature, R is the gas constant, and K_1 and K_2 are constants.

During the late stage of $\gamma \rightarrow \alpha$, the phase transformation follows the site saturation model:

$$\frac{dX_{F_2}}{dt} = K_3 S_\gamma G_F (1-X) \qquad \text{(Eq 3)}$$

where X_{F_2} is the transformed fraction of α at the late stage of the $\gamma \rightarrow \alpha$ transformation, and K_3 is a coefficient that can be determined experimentally.

For continuous cooling, the $\gamma \rightarrow$ P transformation can be described by:

$$\frac{dX_P}{dT} = K_4 S_\gamma G_P (1-X) \qquad \text{(Eq 4)}$$

where X_P is the transformed fraction of $\gamma \rightarrow$ P, G_P is the growth rate of pearlite phase, and K_4 is a coefficient that can also be determined experimentally.

For continuous cooling, the $\gamma \rightarrow$ B transformation can be described by:

$$\frac{dX_B}{dt} = K_5 S_\gamma G_F (1-X) \qquad \text{(Eq 5)}$$

where X_B is the transformed fraction of bainite, and K_5 is a coefficient that can be determined experimentally.

2.2 *Thermodynamic Calculations of ΔG_V and γ/α Equilibrium Temperature, Ae_3*

As the temperature of the steel drops below Ae_3, phase transformation of $\gamma \rightarrow \alpha$ starts. When the equilibrium between γ- and α-phases is reached, the following conditions should be satisfied according to the second law of thermodynamics:

$$\mu_i^{\alpha} = \mu_i^{\gamma} \quad \text{(Eq 6)}$$

where μ_i^{α} and μ_i^{γ} are the chemical potentials of α- and γ-phases, respectively.

When γ-phase is subjected to hot deformation, its energy state increases. This will result in an increase of free energy in the free energy versus chemical composition plots, and the equilibrium condition follows:

$$\mu_i^{\alpha} = \mu_i^{\gamma} + \Delta\mu^d \quad \text{(Eq 7)}$$

$$\Delta\mu^d = \frac{1}{2}\mu b^2 \rho V_{\gamma} \quad \text{(Eq 8)}$$

where μ is the shear modulus of γ-phase, b is the value of Burger's vector, and ρ is the dislocation density (cm^{-2}).

The relations between ρ and hot deformation conditions can be obtained from Ref 5. In the present paper, ΔG_V and Ae_3 were calculated by using the H-S model and the superelement model (Ref 6, 7), respectively.

2.3 *Determination of K_1 to K_4*

Thermodilatometric experiments were performed on a Gleeble-1500 simulator (IBM Corp., White Plains, NY). Values for K_1 and K_4 were obtained from these experimental results. The two steels used in this work were supplied by Bao Steel (China). The analyzed compositions of these steels are 0.087C-1.18Mn-0.168Si-0.03P-0.019S and 0.174C-1.24Mn-0.468Si-0.02S-0.01P (weight percent). The specimens were first reheated from room temperature to 1373 K at a heating rate of 1.8 K/s and then held for 5 min at 1373 K to be fully austenitized. They were then slowly cooled to ambient temperature at a cooling rate of 0.417 K/s. During the slow cooling stage, the radial dilatometric curves of the specimens were measured. These curves correspond to the phase transformations during the slow cooling stage. A typical measured radial dilatometric curve is shown in Fig. 1.

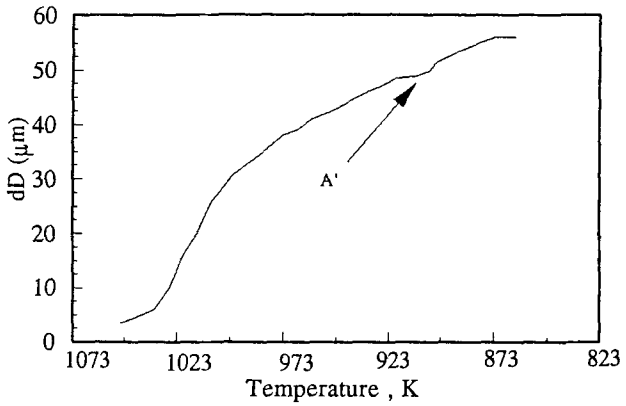

Fig. 1 Typical radial dilatometric curve. Steel chemical composition: 0.087C-1.18Mn-0.168Si-0.03P-0.019S (wt%). A', start point of pearlite transformation

During the progression of transformation from γ-phase, small differences always exist between the actual temperatures of the specimens and the equipment setup temperatures. In the present work, these differences were eliminated by using the irritation correcting method developed by Hawbolt et al. (Ref 8-10). The relation of transformed phase fractions and the corrected dilatometric curve satisfies the following condition:

$$X_i = \frac{\Delta D_i}{D_T} \quad \text{(Eq 9)}$$

where ΔD_i is the corrected magnitude of the radial dilation at different times, and D_T is the corrected magnitude of the total radial dilation.

After further arrangements of Eq 1 and 2, the linear relation of

$$\ln \frac{(dX_F/dt)T^{1/8} D^{-1/4}}{4.046 G_F^{3/4} [\ln 1/(1-X)]^{3/4} (1-X)}$$

and $(4RT\Delta G_V^2)^{-1}$ can be established; its slope and intercept are K_2 and $(\frac{1}{4} \ln K_1 S_{\gamma})$, respectively. By putting the measured transformed phase fractions at the early $\gamma \rightarrow \alpha$ transformation stage ($X \leq 0.2$) into this linear relation, K_1 and K_2 can be calculated. For the two experimental steels, the resulting values of K_1 and K_2 are very close to each other, indicating good accuracy in the experiments. The average values of K_1 and K_2 for the two tested steels are 476,528 cm $\cdot$ $K^{-1/2}$ and 1.14×10^9 J^3/mol^3, respectively.

By inserting the measured transformed phase fractions at the late $\gamma \rightarrow \alpha$ transformation stage into Eq 3, the regression relation of $K_3 S_{\gamma}$ and temperature can be obtained as:

$$K_3 S_{\gamma} = 10.45 + 2.5\left(\frac{1000}{T}\right)^{44.6} \quad \text{(Eq 10)}$$

Inserting the measured transformed phase fractions of $\gamma \rightarrow P$ into Eq 4, we obtained an approximately linear relation between dX_P/dt and $G_P(1-X)$. Its slope is $K_4 S_{\gamma}$, and $K_4 S_{\gamma} \approx 6.0 \times 10^6$ cm^{-1}. The value of K_5 can be obtained from Ref 1.

Table 1 Chemical composition of experimental steels

Steel	Composition, wt %					
	C	Mn	Si	P	S	V
A	0.09	0.5	0.25	0.025	0.02	<0.09
B	0.15	0.8	0.05	0.015	0.03	...
C	0.20	0.58	0.24	0.024	0.019	...

2.4 *Calculation Flow Chart*

In this work, we assume that when the phase transformation rates determined by Eq 1 and 3 become equal, the mechanism of $\gamma \rightarrow \alpha$ transformation will change from the nucleation and growth model to the site saturation model. The start condition of $\gamma \rightarrow$ P transformation can be determined according to Ref 1. When the temperature is below the bainite formation point, B_S, $\gamma \rightarrow$ B transformation occurs. B_S can be obtained from Ref 11. The detailed calculation flow chart is shown in Fig. 2.

2.5 *Pilot Hot Rolling Experiments*

Pilot hot rolling experiments were conducted to verify the computer models. The chemical compositions of the experimental steels are given in Table 1. The controlled rolling and controlled cooling experiments were performed on a Φ300 rolling mill in the National Key Lab for Rolling Technology & Tandem Rolling Automation (Northeast University, China). The size of the slabs was 35 by 100 by 180 mm. Reheating temperature was 1200 °C, and holding time was 30 min. The slabs were hot rolled for four passes; the thickness reduction schedule was 35 → 25 → 15 → 10 → 4 mm. Simulated accelerated cooling was carried out immediately after finishing at different temperatures. At different end-cooling temperatures, the plates were placed in a thermally insulated box to cool to room temperature.

Metallographic samples were cut from the hot-rolled plates. Microstructures in the cross sections vertical to the rolling direction were examined using an optical microscope. The volume fractions of ferrite, pearlite, and bainite were measured with a KAT 386 image analysis system (IBM Corp., White

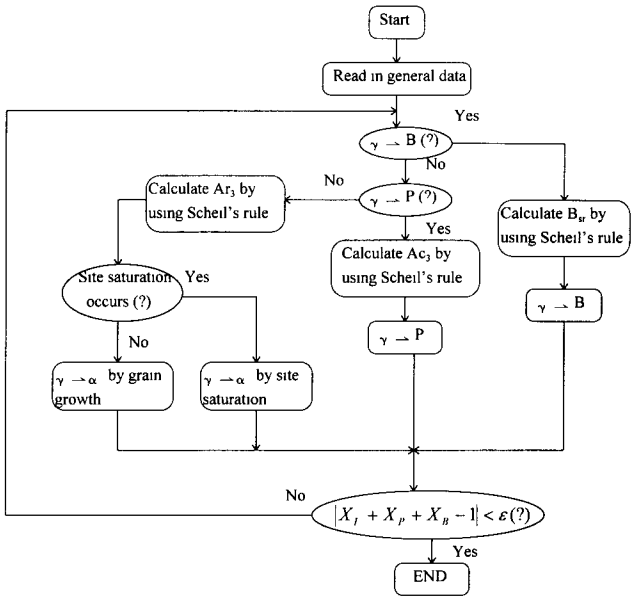

Fig. 2 Computer flow chart for modeling the phase transformation progression

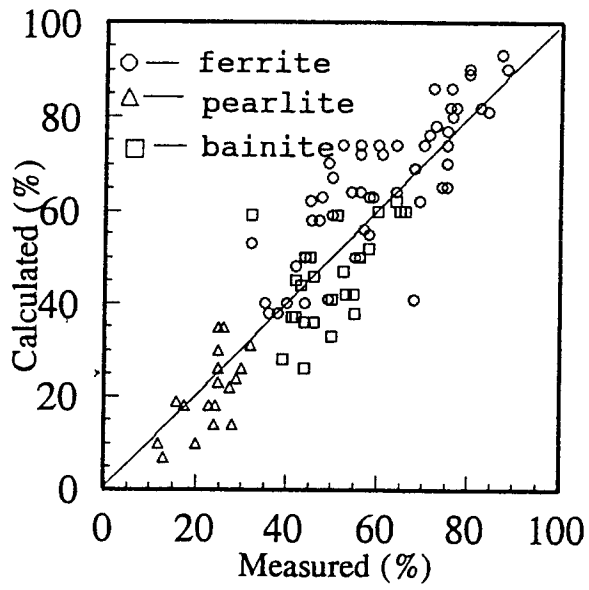

Fig. 3 Comparison of computer-calculated and measured transformed phase fractions in hot-deformed carbon-manganese steels

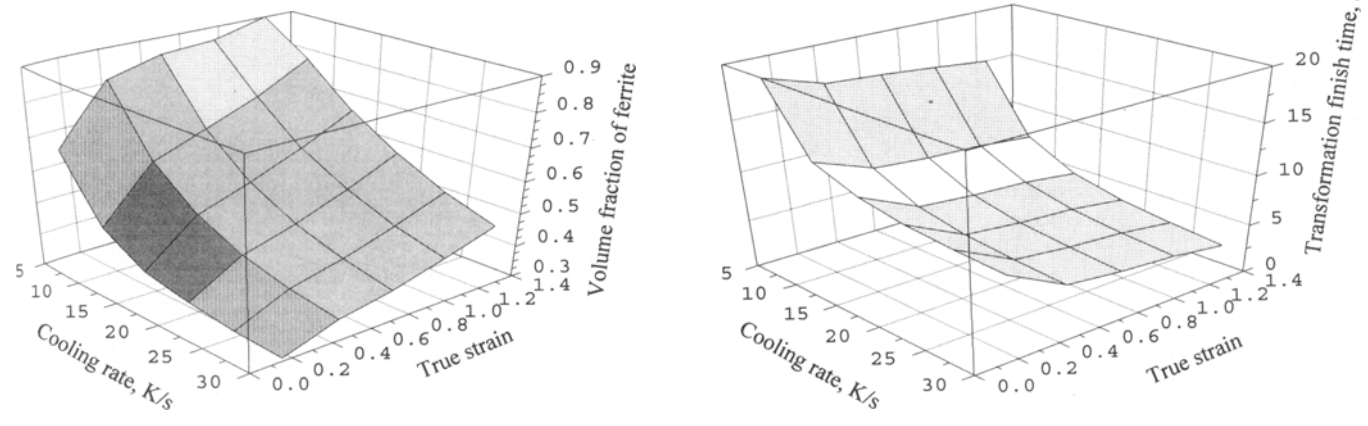

(a) **(b)**

Fig. 4 Relationship between processing parameters and phase transformation behavior predicted by the computer models. (a) Cooling rate and true strain versus transformed α-phase fraction. (b) Cooling rate and true strain versus transformation finishing time

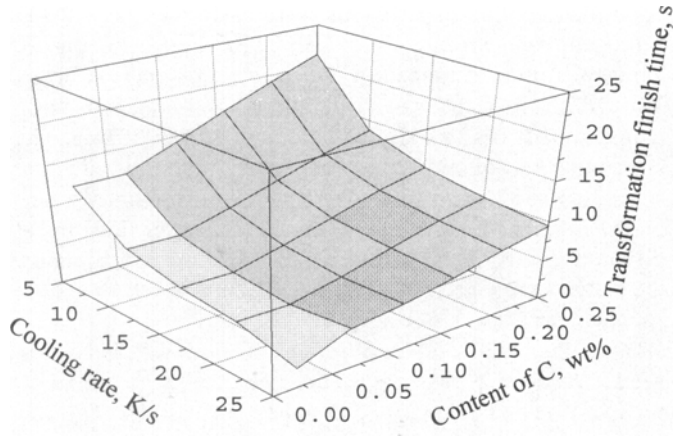

(a)

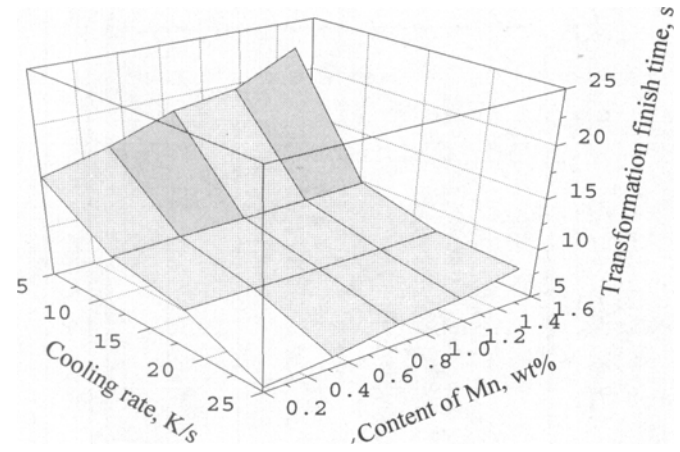

(b)

Fig. 5 Relationship between chemical composition and phase transformation behavior predicted by the computer models. (a) Carbon content and cooling rate versus transformation finishing time. (b) Manganese content and cooling rate versus transformation finishing time

Plains, NY). According to the experimental conditions, calculations were carried out using the models described earlier.

3. Results and Discussion

Before calculating the transformed fractions of α, P, and B, the γ-grain surface area per unit volume, S_γ, should be determined. In this paper, the method developed in Ref 12 was used to calculate changes in γ-grain size during hot rolling. The calculated and measured transformed phase fractions are compared in Fig. 3. The differences between the calculated and measured results are within ±15%, indicating good agreement.

Figure 4 presents calculated results showing the effects of cooling rate and hot deformation conditions on the transformed α-phase fractions and on the transformation finishing time. Figure 4(a) shows that an increase in cooling rate can reduce the volume of α-phase transformed from γ, whereas an increase

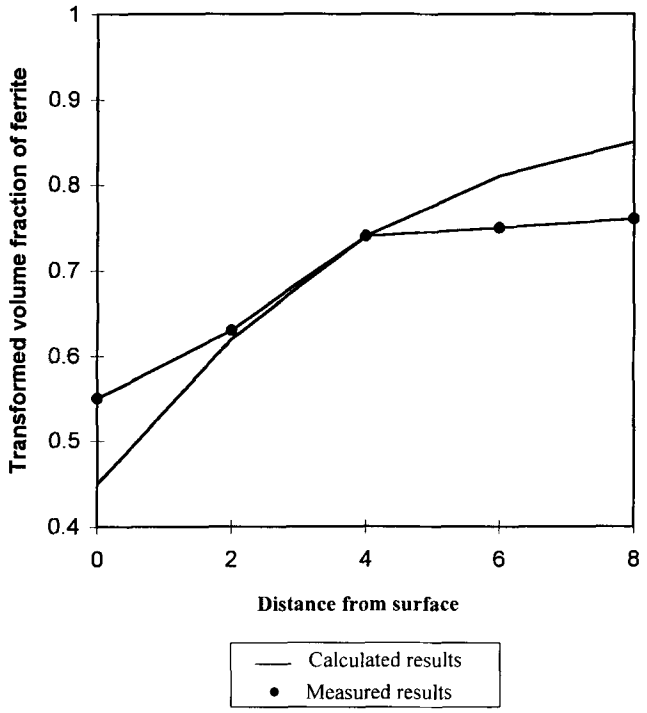

Fig. 6 Calculated and measured distributions of α-phase volume fraction along the cross section of a 16Mn hot-rolled strip (strip gage = 16 mm)

in strain in the γ-phase can promote this transformation. As shown in Fig. 4(b), an increase in either cooling rate or strain in the γ-phase can reduce the transformation finishing time—that is, move the continuous cooling transformation (CCT) curves to the left. These results are consistent with metallurgical principles and experimental observations.

Figure 5 shows the calculated results that describe the effects of chemical composition and cooling rate on the transformation processes. Both the carbon and manganese contents can prolong the transformation finishing time (i.e., move the CCT curve to the right). It should be noted that when the manganese content increased from 0.2 to 1.4 wt% at a cooling rate of 5 K/s, the transformation finishing time changed from 15 to 22.5 s, and increase of 40%. However, the same increase in manganese content changed the transformation finishing time from 0.8 to 4.9 s at a cooling rate of 25 K/s, an increase of 500%. This indicates that manganese content has a much stronger influence on phase transformation when the cooling rate is higher. At relatively high cooling rates, bainite transformation often takes place. Bainite is a mixture of ferrite and carbide. Manganese is reported to be a weak carbide-formation element in steels (Ref 13) and thus may slow the formation of bainite.

With the models described earlier, we calculated the distributions of ferrite volume fractions across the rolling direction of hot-rolled strip produced by BHP New Zealand Steel by using the processing parameters provided in Ref 14. The calculated and measured results are given in Fig. 6; the calculated results showed reasonably good agreement with the results measured by optical microscopy. As shown in Fig. 6, the ferrite volume fraction decreases near the surface area of the hot strip. This is because the cooling rate is high near the surface. Ac-

cording to the earlier discussion, the higher cooling rate will restrain the transformation progress of $\gamma \rightarrow \alpha$.

4. Conclusions

Computer models have been established and used to describe with good precision γ-phase transformation processes in hot-deformed carbon-manganese steels during continuous cooling. These models can be used to analyze the effects of processing parameters (hot deformation and cooling conditions) and chemical composition on the phase transformation kinetics. These models can also provide a foundation for computer simulation of thermomechanical processing of steels, such as controlled rolling and controlled cooling.

Acknowledgment

The authors wish to thank BHP New Zealand Steel for assistance received during the writing of this paper.

References

1. S. Suehiro, *Iron Steel,* Vol 8, 1987, p 10
2. J.W. Cahn, *Acta Metall.,* Vol 34, 1956, p 572
3. E. Scheil, *Arch. Eisenhüttenwes.,* Vol 12, 1935, p 565
4. W.F. Lange, M. Enomoto, and H.I. Aaronson, *Metall. Trans. A,* Vol 19, 1988, p 427-440
5. G. Anan, *Iron Steel Inst. Jpn. Int.,* Vol 32, 1992, p 261
6. Z. Liu, G. Wang, and Q. Zhang, et al., *J. Iron Steel Res.,* Vol 17, 1994, p 128 (in Chinese)
7. Z. Liu, G. Wang, and Q. Zhang, et al., *Acta Metall. Sin (China),* Vol 30, 1994, p 236 (in Chinese)
8. E.B. Hawbolt, *Metall. Trans. A,* Vol 14, 1983, p 1803
9. E.B. Hawbolt, *Metall. Trans. A,* Vol 16, 1985, p 565
10. P.C. Campbell, *Metall. Trans. A,* Vol 22, 1991, p 2791
11. A.K. Jena and M.C. Chaturvedi, Ed., *Phase Transformation in Metals,* Prentice-Hall, 1988, p 443
12. Z. Liu, G. Wang, and Q. Zhang, et al., *J. Mater. Sci. Technol.,* Vol 9, 1993, p 111
13. W.C. Leslie, Ed., *The Physical Metallurgy of Steels,* Hemisphere, 1981, p 175
14. R.J. Hill, "The Effect of Run Out Table Cooling Pattern on the Microstructure and Mechanical Properties of 16Mn Gauge Hot Rolled Coil," Report to BHP New Zealand Steel, University of Auckland, 1994